

Incorporation of protein flexibility and conformational energy penalties in docking screens to improve ligand discovery

Marcus Fischer^{1,2†}, Ryan G. Coleman^{1†}, James S. Fraser^{3*} and Brian K. Shoichet^{1,2*}

Proteins fluctuate between alternative conformations, which presents a challenge for ligand discovery because such flexibility is difficult to treat computationally owing to problems with conformational sampling and energy weighting. Here we describe a flexible docking method that samples and weights protein conformations using experimentally derived conformations as a guide. The crystallographically refined occupancies of these conformations, which are observable in an apo receptor structure, define energy penalties for docking. In a large prospective library screen, we identified new ligands that target specific receptor conformations of a cavity in cytochrome *c* peroxidase, and we confirm both ligand pose and associated receptor conformation predictions by crystallography. The inclusion of receptor flexibility led to ligands with new chemotypes and physical properties. By exploiting experimental measures of loop and side-chain flexibility, this method can be extended to the discovery of new ligands for hundreds of targets in the Protein Data Bank for which similar experimental information is available.

In their native states proteins fluctuate among multiple conformations, and recent evidence from NMR spectroscopy^{1,2} and crystallography^{3–7} suggests apo proteins may transiently populate the conformations adopted in ligand complexes. It is tempting to wonder whether these conformations may be used prospectively to address two long-standing problems in exploiting protein flexibility in ligand discovery⁸: sampling protein states and weighting these states relative to one another^{9,10}.

Sampling protein conformations for ligand discovery is challenging because of the many degrees of freedom available to folded proteins. Conformational changes often involve not only rotamer transitions, but also coordinated loop and main-chain movements. The different internal energies of these conformations affect ligand-binding affinity and, if unaccounted for, high-energy decoy conformations may dominate the docking.

Two strategies have been introduced to model protein flexibility in docking screens for new ligands. ‘Soft docking’¹¹ reduces the steric component of the scoring function and can identify ligands that might be accommodated by certain protein rearrangements. This, however, can increase docking false positives⁹. A related method averages several structures to represent multiple conformations¹². This also reduces the number of states, but suffers from an unphysical averaging of energies, which reduces predictive success¹².

A second strategy explicitly represents, and docks into, multiple receptor conformations^{13–16}. These conformations may be sampled in different ligand complexes^{12,17–21} or calculated using molecular dynamics^{22–26}, elastic network models and related techniques²⁷. Whereas the restriction to experimentally determined conformations ensures accessible states, it limits their number and remains biased to known structures. To calculate alternative conformations from simulations escapes such biases, but struggles to access states separated by barriers of higher energy. Neither approach easily assigns energy penalties to the different

conformations, and several studies have found that using too many conformations in flexible docking can reduce the enrichment of known ligands over decoy molecules^{9,28–32}.

Recent advances in crystallographic refinement offer the opportunity to model higher-energy conformational states using direct experimental observations^{3–5,33–35}. Such alternative conformations can be discovered in weak electron-density features and reliably modelled at lower occupancies than the dominant conformation^{3,34,35}. A liability of this approach is its inability to identify confidently the conformations present at less than ~10% of the ground state, or no more than about 2 kcal mol⁻¹ higher in energy at room temperature. It can represent coordinated transitions as easily as changes in side-chain rotamers, and the relative conformational energies emerge directly from crystallographic occupancies.

Here we explore the use of multiple conformations present in the electron-density map of an apo cavity site in cytochrome *c* peroxidase (CcP)^{36–39} in docking screens. The substitution Trp191 → Gly in CcP creates an enclosed anionic cavity of about 200 Å³, which has been studied as a model site for ligand binding. In the variant studied here, residues 192–193 have been deleted, and the substitution Pro190 → Gly introduced, which increases the flexibility of the cavity’s gating loop. In the room-temperature structure that we determined to 1.57 Å resolution, one loop and three side chains of this ‘gateless’ cavity occupy multiple states in the electron density. We docked 583,363 compounds against 16 energy-weighted conformations of the cavity. To limit the calculation cost, we modified the treatment of ligand–protein electrostatic interaction energies to decompose them into an additive function⁴⁰. This allowed us to sample 16 receptor states with only a 2.4-fold speed cost compared with that of a single structure. From the flexible docking screen, 15 new compounds were chosen to test, and ten of these were confirmed to bind. The crystal structures of nine of them were determined, which allowed us to compare predicted and

¹Department of Pharmaceutical Chemistry, University of California San Francisco, San Francisco, California 94158, USA, ²Faculty of Pharmacy, Donnelly Center, University of Toronto, 160 College St, Toronto, Ontario M5S 3E1 Canada, ³Department of Bioengineering and Therapeutic Sciences, University of California San Francisco, San Francisco, California 94158, USA; [†]These authors contributed equally to this work.

*e-mail: james.fraser@ucsf.edu; bshoichet@gmail.com

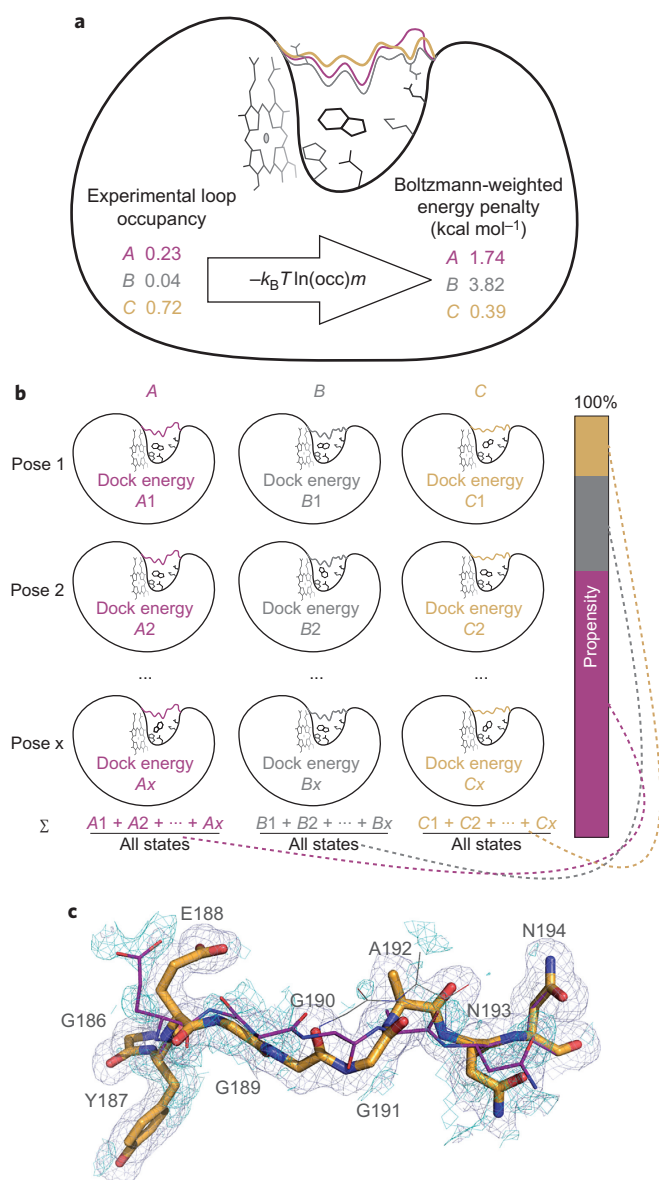


Figure 1 | Experimental occupancies of apo loop conformations set the penalties for docking. **a**, From experimental loop occupancies to docking penalties. Flexible loop (in colours) and side-chain conformations of the apo CcP gateless protein are assigned Boltzmann-weighted energy penalties based on their crystallographic occupancy (here $m = 2$). **b**, From docking energies to loop propensities. The Boltzmann sum of the energies of all x poses for a ligand to different loops A , B and C are calculated. The result is expressed as a percentage, which indicates the predicted preference of the ligand to bind to a particular loop conformation and can be compared to the experimental occupancies. **c**, Electron density shows evidence for three conformations of the apo loop, with the missing conformation of loops A (purple sticks) and B (grey lines) when only loop C (orange sticks) is included in the refinement shown as blue ($2mF_o - DFC$, 1σ) and cyan ($F_o - F_c$, $+1.5\sigma$). The stick radius is according to relative occupancies (see Fig. 2a). See Supplementary Fig. 13 for a more-pronounced difference map density for loop B when including A in addition to C in the refinement.

observed ligand poses and loop structures. The potentials for a broad application of this method are considered.

Results

From crystallographic occupancies to Boltzmann-weighted energy penalties. Our first goal was to convert crystallographic

occupancies for the flexible 186–194 loop into Boltzmann-weighted energy penalties for docking (Fig. 1 and Supplementary Fig. 2). This loop adopts three conformations in previously determined ligand-bound structures³⁹. These three states, which we designate as A , B and C , were combined into a multiconformer loop model. Occupancy refinement of these conformations, using the apo structure electron density, improved the agreement between the model and experimental data as judged by R_{free} values that ranged from 0.1639 to 0.1695 (Supplementary Table 2) and qualitatively fit the density (Fig. 1c).

We used the refined apo occupancies of each loop conformation to assign energy penalties to each conformation (see Fig. 1) using equation (1):

$$\text{energy penalty (conformation } A) = -k_B T \ln(\text{occ}(A))m \quad (1)$$

with k_B = Boltzmann constant, T = temperature (K), occ = occupancy, m = flexible weighting multiplier (see below). The occupancy of loop B dropped below 10% (Fig. 1), which we consider the imprecision of the refinement approach. Although refinement parameters can affect the occupancy, our procedure converged to 4% after ten refinement cycles, remained stable thereafter (Supplementary Fig. 2) and could be reproduced from another dataset (Supplementary Fig. 3). Also, the loop can move freely and is unobstructed by crystal contacts (Supplementary Fig. 11). In the Supplementary Information, we address the robustness and dependence of the results on the exact numerical occupancy value.

Retrospective testing and integration of conformational weights and docking scores. To test the usefulness of these energy penalties, we retrospectively docked five known cavity ligands with the new scoring function (compounds 1–5 (Table 1)) and recovered experimental poses for three of them with an average root-mean-square deviation (RMSD) of 0.4 Å (Supplementary Fig. 4).

A more stringent test compares not only the docked and observed ligand poses, but also the predicted and observed ensemble of protein conformations associated with each pose. If the energy weightings of the apo loop conformations are correct, we can combine them with docking scores to predict the distribution of conformations favoured for each ligand complex. Predicted loop propensities (analogous to experimental occupancies) were calculated, using equation (2), as the Boltzmann sum of the energy of all ligand poses bound to a specific loop conformation $X = (A, B \text{ or } C)$ over the Boltzmann sum of the energy of all the poses generated to any loop (Supplementary Methods and Supplementary Table 4):

$$\text{propensity}_{\text{ligand } Z, \text{loop } X} = \frac{\sum_{x \in \text{loop } X} e^{\text{dock energy}(x, Z)/kT}}{\sum_{y \in \text{all states}} e^{\text{dock energy}(y, Z)/kT}} \quad (2)$$

Docking energies are computed by DOCK3.7⁴¹ according to equation (3), which integrates the receptor energy penalties from equation (1):

$$\text{dock energy (loop } X, \text{ ligand } Z) = \text{energy penalty(loop } X) + \sum_{\text{atom } z \in \text{ligand } z} \text{Vdw}(z) + \text{elstat}(z) + \text{ligand desol}(z) \quad (3)$$

Here the energy penalty is from equation (1), $\text{Vdw}(z)$ is the van der Waals energy of each ligand atom⁴², $\text{elstat}(z)$ is the corresponding electrostatics energy⁴³ and $\text{ligand desol}(z)$ is the ligand desolvation energy. The resulting propensities are expressed as a percentage, with all propensities for a ligand summing to 100% (Fig. 1b).

With the predicted loop occupancies for the holo complexes calculated from the apo state docking and loop propensities, we refined the observed loop occupancies against five ligand-complex datasets, determined to between 1.2 and 1.7 Å (Supplementary Table 1). This

Table 1 | CcP ligands: previously discovered (1-5) and found by flexible docking (6-20).

Rank	ZINC	No.	Compound	Ligand RMSD (Å)*	Loop state† Xtal / DOCK (PCC‡)	Affinity (μM) / ligand efficiency (kcal mol ⁻¹ hac ⁻¹)	Max T _c to known ligands§	Closest known ligand§	Closest known affinity (μM)
n.a.	01583444	1		n.a.	C (n.a.)	n.d.	1	Is known	n.a
n.a.	00331902	2		n.a.	A (n.a.)	33 (0.68)	1	Is known	n.a
n.a.	00331945	3		n.a.	AB (n.a.)	3 (0.69)	1	Is known	n.a
n.a.	00036634	4		n.a.	A (n.a.)	9 (0.77)	1	Is known	n.a
n.a.	08652421	5		n.a.	B (n.a.)	106 (0.78)	1	Is known	n.a
8	06656163	6		0.88	C / B (-0.78)	71 ± 10 (0.35)	0.48		19 (ref. 37)
38	04962659	7		0.48	B / B (0.85)	8 (0.35) (ref. 37)	1	Was known* (ref. 37)	8 (ref. 37)
70	00331160	8		0.48	B / B (1.00)	19 (0.54) (ref. 37)	1	Was known* (ref. 37)	19 (ref. 37)
163	13739037	9		0.98	C / C (0.88)	n.b.d. <4 mM	0.29		288 (ref. 37)
322	01596053	10		0.79	AC / A (0.41)	22 ± 10 (0.4)	0.53		41 (ref. 39)
330	34979991	11		1.19	A / A (0.99)	46 ± 8 (0.46)	0.28		33 (ref. 39)
433	00203341	12		1.49	A / A (0.62)	28 ± 7 (0.44)	0.30		8 (ref. 37)
526	00519712	13		0.54	AC / A (0.61)	7 ± 0.6 (0.47)	0.36		19 (ref. 37)

Continued

Table 1 | (continued)

Rank	ZINC	No.	Compound	Ligand RMSD (Å) ^a	Loop state [†] Xtal / DOCK (PCC [‡])	Affinity (μM) / ligand efficiency (kcal mol ⁻¹ hac ⁻¹)	Max T _c to known ligands [§]	Closest known ligand [§]	Closest known affinity [¶] (μM)
556	00388812	14		0.55	BC / C (0.49)	23 ± 4 (0.49)	0.23		64 (ref. 37)
67	70974074	15		n.a.	/ C	n.r.	0.27		203 (ref. 37)
84	16210033	16		n.a.	/ C	n.b.d.	0.31		33 (ref. 39)
263	19702757	17		n.a.	/ B	n.d.	0.35		19 (ref. 37)
355	12546268	18		n.a.	/ A	396 ± 42 (0.42)	0.37		14 (ref. 37)
401	16207704	19		n.a.	/ C	n.b.d.	0.31		33 (ref. 39)
487	01648614	20		n.a.	/ A	n.r.	0.20		19 (ref. 37)

^aLigand heavy atom RMSD between docked pose and crystal pose. [†]Dominant loop state listed unless two states within 10% of maximum, when both are listed. [‡]PCC of loop occupancies versus predicted loop propensities from docking. [§]Extended connectivity fingerprints (ECFP4), ligand with this Tanimoto shown at the right. [¶]Determined previously; references in parenthesis. n.a., not applicable; n.b.d., no binding detectable (because precipitation >500 μM if not specified otherwise); n.d., not determined (insufficient solubility); n.r., not reproducible in repetitive runs.

yields a distribution of loop conformations for complexes (Supplementary Fig. 5). Overall, conformation-weighted docking correctly predicted the dominant loop state for all five ligands (Supplementary Fig. 5), with an overall Pearson correlation coefficient (PCC) of 0.77 (for three loop states for all five ligands) (Supplementary Fig. 6).

In calculating the propensity of the loop conformation for the individual ligand complexes, we add the ligand docking-energy score to the occupancy-based loop energies (equation (3)). As these loop energies are rarely on the same scale as the docking score, the combination of the two terms can be optimized. We investigated weighting the conformation energies (m in equation (1)). To reduce the dangers of overfitting, we established retrospectively a single-variable weighting term (m) of 2 (performance was judged by the increase in statistical significance over other integers (Fig. 2, Supplementary Figs 5 and 6a, and Supplementary Methods).

As experimental occupancies can be imprecise and covary with B-factors, which model the fall-off of the density from the mean position, we investigated how the results depended on refined loop occupancies (see Supplementary Methods). The effect on the retrospective propensities was minor and correlations between the predictions and experiments remained significant (Supplementary Figs 6c and 10b). This gives confidence that the energy penalization is not overly sensitive to the input occupancy of low-occupancy states like

loop B, which is comforting in terms of the expected error in the determination and refinement of experimental occupancies.

Prospective docking for new ligands that complement the different receptor conformations. Fortified by these results, we used this energy-penalized ensemble of flexible states for the prospective docking of 583,363 fragments from the ZINC database⁴⁴. From the top 0.1% of the highest-ranking molecules, 15 were chosen for experimental testing (compounds 6–20 (Table 1)). As is common in selecting docked molecules to test experimentally from the docking hit list^{45,46}, we eliminated compounds that had problems with protonation or tautomerization states, and selected several molecules for chemical novelty, including some uncharged molecules. We particularly sought molecules predicted to bind to different protein–receptor conformations.

On testing, nine of the 15 compounds had K_d values between 7 and 400 μM as measured by the haem Soret-band shift (Table 1). The ligand efficiencies were between 0.35 and 0.54 kcal mol⁻¹ per heavy atom count (hac). For eight of these nine molecules we determined the X-ray crystal structures, and we also determined a structure for a tenth molecule for which we had been unable to determine an affinity. The nine ligand crystal structures recapitulated the predicted docked ligand poses (Fig. 3), with a mean RMSD of 0.82 Å (Table 1). Counting ligand binding by affinity

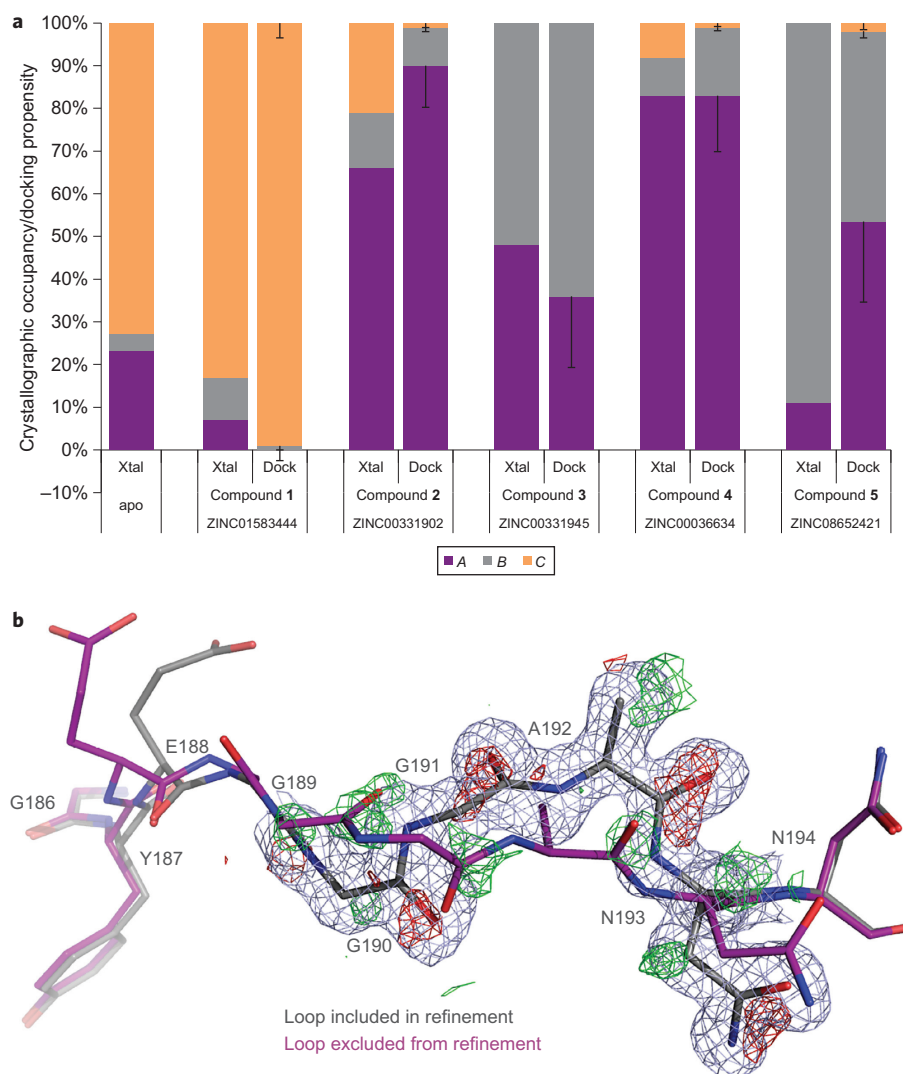


Figure 2 | Predicting loop occupancies in holo complexes. **a**, Experimental occupancies of the three flexible loop (186–194) conformations *A*, *B* and *C* are depicted as a percentage (Xtal). These can then be compared easily to their predicted docking propensities (dock) for compounds **1–5**⁴⁴. Using Boltzmann-energy penalties and a multiplier $m = 2$ results in close agreement of the major loop conformation between prediction (dock) and experiment (Xtal), with a PCC of 0.83 and a P value < 0.01 . Error bars for docking propensities are derived by using any flexible weighting multiplier m between 1.0 and 3.0 and taking the standard deviation. The error bars are symmetric in both the up and down direction; the up direction has been omitted for clarity. **b**, The difference electron-density map of CcP and compound **5** around the backbone carbonyls (red mesh for the main loop in grey sticks and green for the new loop conformation) provides evidence for the presence of a second loop conformation (purple) even at very low levels of around 10%. Resolution is 1.2 Å; 2mFo-DFc map (blue mesh) rendered at 1σ and mFo-DFc (red and green mesh) map at 2.6σ .

and by crystallography, the total hit rate was 67% (10/15). The new hits differed from previously known ligands: the highest pairwise topological similarity to these, using ECFP4-based Tanimoto⁴⁷ coefficients, was 0.36 (Supplementary Table 9), and new ligands were, on average, 52 Da heavier (from 148 to 200 Da) than the previously known ligands, and also larger than those discovered in an earlier rigid-body docking study³⁷. A role of human selection of compounds, in both the previous docking studies and in this one, cannot be entirely controlled for.

When writing this manuscript we discovered that two of the 15 molecules (**7** and **8**) had been found independently in work that was then unpublished³⁷; we do not count these as novel molecules. They do, nevertheless, illustrate the strength of the method. Of all the new ligands, **7** and **8** most closely resemble the earlier series of cavity ligands and, indeed, were predicted and observed to prefer the *B* loop conformation, which has been previously targeted in the older rigid-docking method.

Ligands select the predicted protein loop and side-chain conformations. A crucial point is the ability of the method to anticipate the protein conformational response to the new ligands. In seven of nine new holo structures, the predicted loop occupancies and conformations corresponded qualitatively to the observed ones, with at least the dominant loop being predicted correctly and frequently to the approximate ratios of the ensemble (Figs 3 and 4). For instance, compound **7** was experimentally observed to bind to loop *B* at 79% (with 20% occupancy of loop *A*), and was predicted to prefer loop *B* at 95% with a 5% loop *A* contribution. For compound **8** the prediction of loop conformations *A* and *B* at 33% and 67%, respectively, agrees quantitatively with the observed holo occupancies at 38% and 62%, respectively. The experimental occupancy of the *C* loop in the complex with compound **9** was 68% instead of the 100% predicted. Compound **11** bound primarily to loop *A* with an occupancy of 84% and the remaining occupancy was split

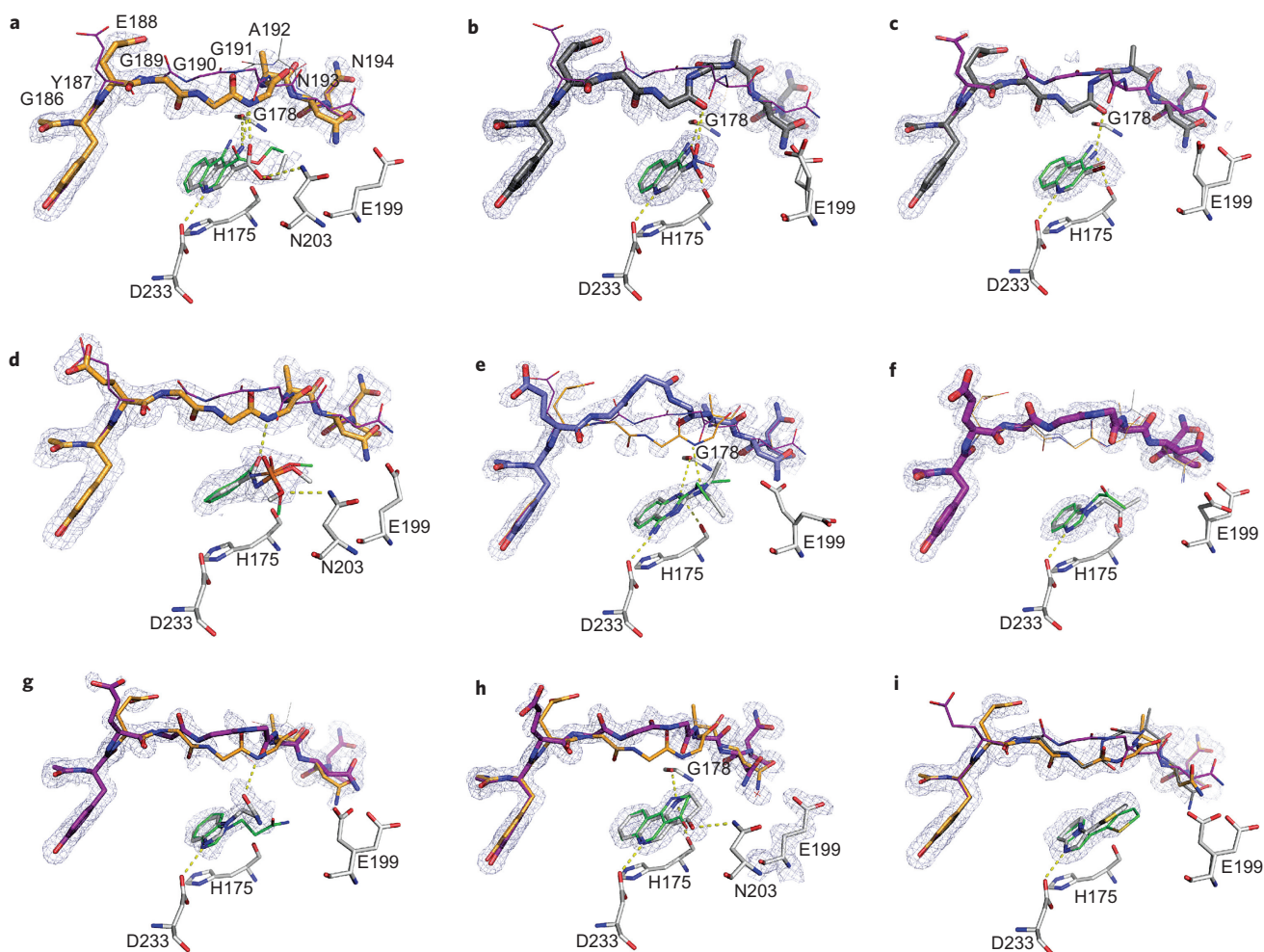


Figure 3 | Experimental binding poses versus prospective docking predictions. The electron density at 1σ is shown for ligand and loop conformations. The loop-stick thickness corresponds to experimentally observed occupancies; the colouring is as before with loop conformation A in purple, B in grey, C in orange and D (for compound 10) in blue. **a–i**, Superposition of the ligand poses, with experimental in grey versus docked in green: compound **6** (**a**), **7** (**b**), **8** (**c**), **9** (**d**), **10** (**e**), **11** (**f**), **12** (**g**), **13** (**h**) and **14** (**i**). For clarity, co-crystallized MES for compounds **6**, **9** and **12** is omitted.

between the additional loops; the prediction was 89% for loop A, which corresponds to a PCC of 0.99. Compound **13** was among the few compounds predicted to bind to one loop conformation exclusively, the A loop. Whereas automatic occupancy refinement suggests a presence of loop C, this may be misled by nearby water molecules, as visual inspection of the electron density seems consistent with only the single A loop being present (Fig. 3). Compound **14** was chosen to bind to an ensemble of loop conformations: 29% loop A, 11% loop B and 60% loop C. The refined experimental occupancy values were consistent with these predictions, with 27% loop A, 30% loop B and 43% loop C, which correspond to a PCC of 0.84. For ligand **10**, a fourth loop conformation was found that had not been modelled previously. To check for this conformation, D, in the apo structure, it was included as a fourth loop in the original model and refined as before, but could not be observed at any reliable level; this represents a false negative of our method (also see Supplementary Fig. 1 and Supplementary Table 7). Meanwhile, the prediction of side-chain conformations conformed to those observed crystallographically with only two failures out of the total 27 modelled conformations (Supplementary Methods and Supplementary Fig. 7). Finally, for several complexes the presence of 2-(*N*-morpholino)ethanesulfonic acid (MES), which itself is a weak ligand, prevented a full analysis of the results (Supplementary Table 8).

Overcoming the bias of known structures: the correct model does not necessarily result in the best retrospective enrichment. It is important to understand whether flexible receptor docking improved the results over standard rigid docking. We first investigated the ranks of the new ligands against both our fully flexible model and any individual loop model. No single model would have ranked all these ligands in the top 0.1% of the database as the flexible docking had (Supplementary Table 5). Had we docked prospectively against all conformations and combined the top-ranking ligands, the hits against the high-energy, low-occupancy B conformation would have dominated, as in previous screens^{37,39}, and the calculation would have taken sevenfold longer.

This bias emerges even more strongly in retrospective screens of all previously known ligands. Such retrospective enrichment is widely used to judge docking performance and to select receptor structures for prospective docking. On that basis we would have selected the B loop, which dominated enrichment plots, and discarded the other conformers (Fig. 5a and Supplementary Table 6). Choosing the best enriching structure in retrospective studies for prospective screens seems intuitive, but it is biased by the binding of most known ligands to the B loop; they were, in fact, discovered by docking to that loop conformation. Compared with ligands that we ourselves had discovered against the single B-loop conformation, the new ligands that bind to the C- and A-loop conformations are

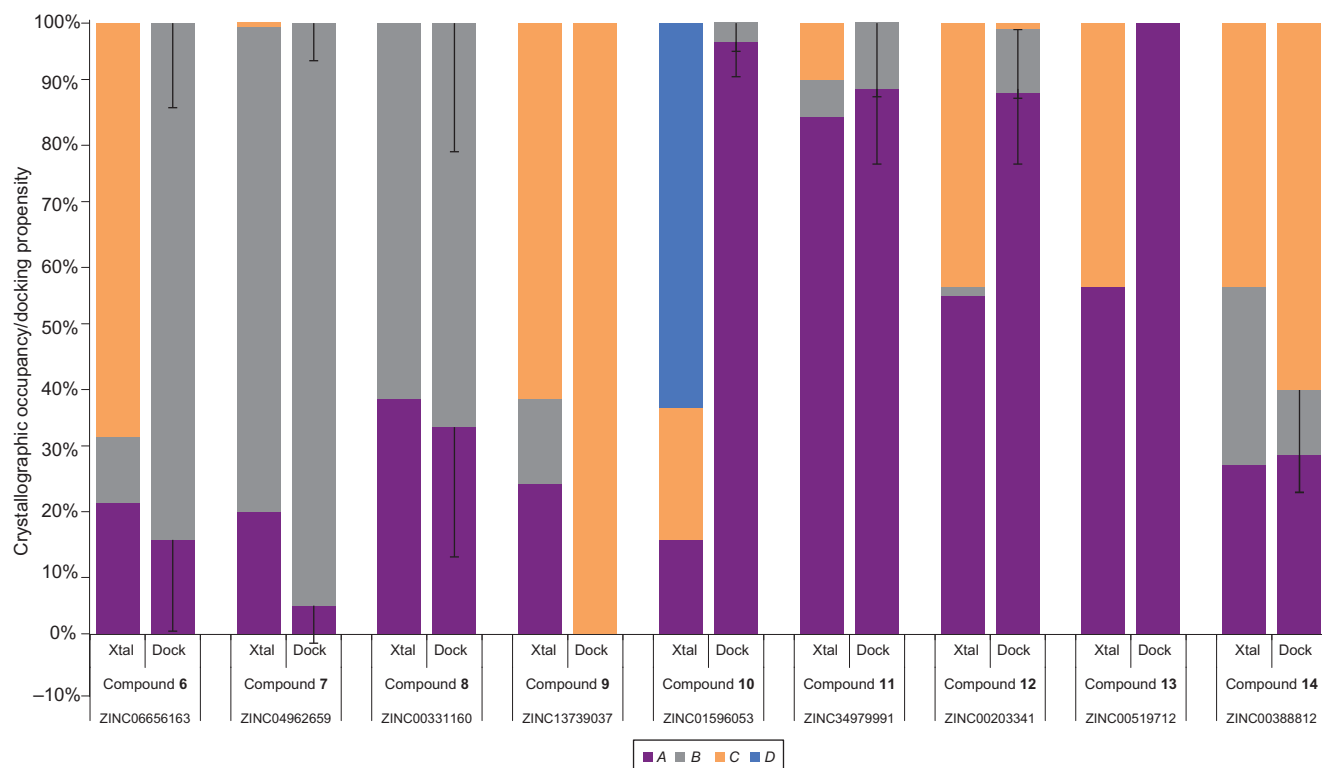


Figure 4 | Predicting loop occupancies in bound complexes. The loop occupancies and predicted propensities for compounds 6–14 are shown, with crystallographic occupancies at the left and predicted loop propensities (with $m = 2$) at the right for each pair. Error bars for the loop propensity represent the standard deviation of the occupancies by varying the flexible weighting multiplier m from 1 to 3. The major loop conformation is predicted correctly for all cases but compound 10, which prefers a fourth loop (D) conformation that was not modelled; compounds 6 and 12 have a larger C loop presence because of the partial presence of MES. The error bars are symmetric in both the up and down direction; the up direction has been omitted for clarity.

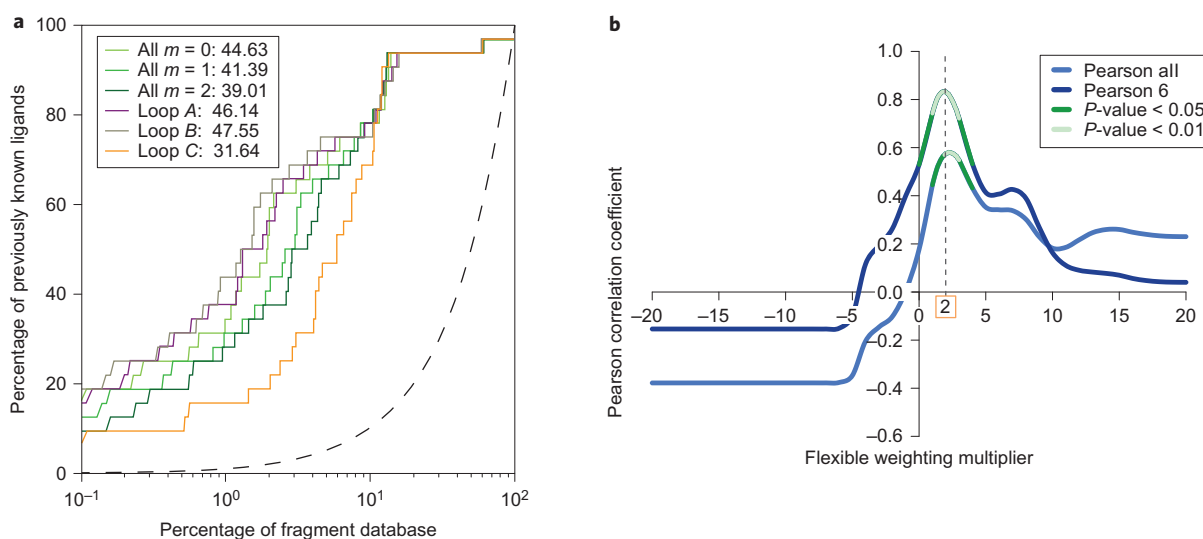


Figure 5 | Enrichment alone cannot distinguish first-in-class from best-in-class. **a**, Retrospective enrichment of known ligands against decoys (adjusted log AUC (area under the curve)) for loops A, B and C individually (coloured as purple, grey and orange, respectively) and combined with different multipliers (tones of green). The adjusted area under the log ROC plot (ROC = receiver operating characteristic) is shown in the key (see Supplementary Table 6 for other common performance metrics). **b**, Pearson correlation of experimental and predicted loop occupancies with statistically significant areas highlighted in green (dark green for P values < 0.05 , light green for $P < 0.01$). Pearson all is for all nine compounds; Pearson 6 is the correlation only considering compounds 7, 8, 9, 11, 13 and 14, for which the results are not distorted by a partial presence of MES.

more diverse and are larger (Supplementary Table 9); they would not have been discovered using the highest enriching model alone (Supplementary Table 4) or, if so, for the wrong reasons (Fig. 5b and Supplementary Fig. 8).

It is appropriate to ask whether this method (dependent as it is on experimental density features) can be used on biorelevant targets. On examining the Protein Data Bank (PDB)⁴⁸ for projects that our flexible docking method could be applied to, we found

827 unique proteins with electron-density maps determined to <1.5 Å resolution, a level substantially more conservative than the 2 Å we estimate required for confident occupancy fitting (Supplementary Methods and Supplementary Fig. 12). Although only 51 of these were determined at room temperatures, as the apo cavity structure was, analysis of an apo cavity structure determined at cryogenic temperatures suggests that much of the flexibility exploited here remains even at these lower temperatures, but there were also important differences (described more fully in the Supporting Information). Although room-temperature structures more fully explore conformational heterogeneity present in protein structures⁴, probably even cryogenic structures have enough conformations to support this analysis.

Discussion

Three principal observations emerge from this study. First, partial occupancy conformations, apparent in electron density from room-temperature crystal structures, enable the modelling of alternative protein conformations in molecular docking. These features not only illuminate conformations accessible to ligands, but their occupancies provide energy weights for the docking scoring function, which prevents domination by higher-energy conformations. Multiple conformations may be represented with only a modest impact on the docking calculation time. Second, exploitation of these conformations enables the prospective prediction of ligands with new chemotypes and new physical properties, with close correspondence between the predicted ligand poses and protein-loop conformations and those subsequently determined by X-ray crystallography. Finally, there are over 800 unique proteins in the PDB, each with the requisite density maps, to which this method could be applied today (see Supplementary Data: possible protein targets).

We were surprised at the high correspondence between the loop propensities and ligand geometries from predictions and those in the X-ray structures of the new complexes. With the exception of the complexes with compound **6** and with compound **10**, the observed loops and residue conformations matched well those predicted, as judged by their relative occupancies and the correct prediction of the major loop conformation (Figs 2 and 4). For six of the nine structures, the occupancies not only corresponded qualitatively, but did so quantitatively as well, with PCCs greater than 0.6 (compounds **7–9** and **11–13**). This suggests that experimental conformational energy weights and docking scores may be in at least a qualitative balance, and may be combined pragmatically. Indeed, the method predicts loop occupancies 30% better than a naive method, which presumes all states to be equi-energetic (Fig. 5b). To check whether the loop-propensity prediction could have been achieved using only ligand similarity, we compared the topological similarity of the 14 known ligands with the correlation of their loop occupancies. Many topologically dissimilar ligands bound to the same major loop conformations (Supplementary Fig. 9), which suggests an advantage of structure-based methods over similarity-based methods alone.

Certain caveats merit discussion. Only a narrow range of conformations above the ground state can be observed reliably in this method. Even here, the *D* conformation of the 186–194 loop, observed in the complexes of ligand **10**, was unanticipated because it was not observed in the apo structure. Whereas the conformational occupancies and the docking propensities were, overall, in balance, there is no fundamental reason why they should be in balance, or that the weighting found here should extend to other systems. The weights assigned based on the occupancies may be converted into energies, but the docking scores, even when physics-based, leave out important terms and make substantial approximations. As docking scoring functions develop to better model physical forces, these terms should come into the balance more reliably than we, perhaps fortuitously, found here.

Conclusions

Notwithstanding the caveats discussed above, this method had important successes. Partial occupancy modelling enabled the representation of alternative, energy-weighted protein conformations that could be integrated with molecular docking scores. This prevented domination by higher-energy conformations in the docking, which might fit ligands better, but at the cost of higher internal energies. Although the number of conformational states grows exponentially, the multiconformer receptor potentials could be recombined in a way that leads to only a modest impact on the docking calculation time. Exploitation of the new conformations illuminated ligands with new chemotypes and new physical properties, and we observed a close correspondence between the predicted ligand poses and protein-loop conformations with those determined subsequently by X-ray crystallography. There are well-over 800 unique proteins to which this method could be applied today.

Methods

The protein was purified and crystallized as described³⁹, with the exception of the apo protein that was crystallized in 100 mM KPi, pH 6.0. A loop model was generated from three main loop conformations (residues 186–194) observed in holo complexes³⁹ with compounds **4**, **5** and apo for loops A, B and C, respectively, and subjected to occupancy refinement (strategy = individual_adp + occupancies) within PHENIX.REFINE³³ in which ten cycles were found to result in sufficient convergence of the loop occupancy (Supplementary Fig. 2). These models are deposited at the PDB as 4NVA–4NVO and 4OQ7 (Supplementary Table 1). Experimental affinities were measured by fluorescence monitoring of the haem Soret-band shift as before^{37,39}.

Flexible receptor preparation. DOCK 3.7⁴¹ uses physics-based scoring that consists of van der Waals⁴² and ligand-desolvation terms⁴⁹, combined with interaction electrostatics using a probe–charge implementation of the Poisson–Boltzmann (PB) equation. The first two components of this score can be broken down independently of the atom, so the receptor can be separated into invariant and flexible parts, with separate scoring grids constructed and then used during docking. For PB electrostatics, the scoring cannot be deconstructed into separate protein components as easily. Here we use QNIFFT^{43,50} on separate but complete receptor conformations. To use these during docking, the PB map of each receptor conformation is compared with the PB of the most-occupied receptor conformation, and the difference maps for the overall conformation are used in docking to construct the overall electrostatic score. This results in a much better approximation to the PB map of a single conformation (see Supplementary Methods). Given a structure with defined flexible regions and occupancies, docking preparation takes place automatically. Both the scripts to do so and the DOCK3.7 code itself are available, without charge, for academic research at <http://dock.compbio.ucsf.edu/DOCK3.7/>

Flexible receptor docking. Several changes were made to the DOCK 3.7 code to enable flexible docking. Each ligand pose is scored against each part of the receptor conformation (here, two residues with two positions each and three loops plus a loop with a residue moved, plus an invariant grid), and nine grids were scored for each ligand pose. The scores were assembled into the $2 \times 2 \times (3 + 1) = 16$ possible cavity conformations and the top score for each was saved, as were the top ten overall poses to any conformation to calculate the receptor conformational propensities. Additional analyses were performed with an implementation of the black-box reweighting algorithm (BBRW)⁵¹ in place of equation (2) (Supplementary Table 3). The code for equation (2) and the BBRW algorithm is included in the DOCK 3.7 distribution (<http://dock.compbio.ucsf.edu/DOCK3.7/>). For the screen of the 583,363 ZINC⁴⁴ fragments, flexible docking took 1,516 core hours spread across 850 nodes, or less than two hours of wall time. Docking a single cavity conformation took 630 hours, only a 2.4-fold computation cost versus a 16-fold increase in conformations sampled.

Accession codes. Crystal structures are available at the PDB (Supplementary Table 1). The structures have the following primary accession codes, in which the numbers in parenthesis designate the ligand that is bound to CcP, and ‘apo_RT’ and ‘apo_cryo’ refer to apo forms of CcP at room temperature and at cryogenic temperature: 4NVA (apo_RT), 4NVB (5), 4NVC (4), 4NVD (3), 4NVE (2), 4NVF (1), 4NVG (6), 4NVH (7), 4NVI (8), 4NVJ (9), 4NVK (10), 4NVL (11), 4NVM (12), 4NVN (13), 4NVO (14) and 4OQ7 (apo_cryo).

Received 16 December 2013; accepted 11 April 2014;
published online 25 May 2014

References

1. Baldwin, A. J. & Kay, L. E. NMR spectroscopy brings invisible protein states into focus. *Nature Chem. Biol.* **5**, 808–814 (2009).

2. Koveal, D., Clarkson, M. W., Wood, T. K., Page, R. & Peti, W. Ligand binding reduces conformational flexibility in the active site of tyrosine phosphatase related to biofilm formation A (TpbA) from *Pseudomonas aeruginosa*. *J. Mol. Biol.* **425**, 2219–2231 (2013).
3. Burnley, B. T., Pavel, V. A., Paul, D. A. & Piet, G. Modelling dynamics in protein crystal structures by ensemble refinement. *eLife Sci.* **1**, e00311 (2012).
4. Fraser, J. S. *et al.* Hidden alternative structures of proline isomerase essential for catalysis. *Nature* **462**, 669–673 (2009).
5. Fraser, J. S. *et al.* Accessing protein conformational ensembles using room-temperature X-ray crystallography. *Proc. Natl Acad. Sci. USA* **108**, 16247–16252 (2011).
6. Frauenfelder, H., Petsko, G. A. & Tsernoglou, D. Temperature-dependent X-ray diffraction as a probe of protein structural dynamics. *Nature* **280**, 558–563 (1979).
7. Rauh, D., Klebe, G. & Stubbs, M. T. Understanding protein–ligand interactions: the price of protein flexibility. *J. Mol. Biol.* **335**, 1325–1341 (2004).
8. Jorgensen, W. L. Rusting of the lock and key model for protein–ligand binding. *Science* **254**, 954–955 (1991).
9. Nicholls, A. The character of molecular modeling. *J. Comput. Aid. Mol. Des.* **26**, 103–105 (2012).
10. Barril, X. & Fradera, X. Incorporating protein flexibility into docking and structure-based drug design. *Expert Opin. Drug Disc.* **1**, 335–349 (2006).
11. Jiang, F., Lin, W. & Rao, Z. SOFTDOCK: understanding of molecular recognition through a systematic docking study. *Protein Eng.* **15**, 257–263 (2002).
12. Cosconati, S. *et al.* Protein flexibility in virtual screening: the BACE-1 case study. *J. Chem. Inf. Model.* **52**, 2697–2704 (2012).
13. Rueda, M., Totrov, M. & Abagyan, R. ALIBERO: evolving a team of complementary pocket conformations rather than a single leader. *J. Chem. Inf. Model.* **52**, 2705–2714 (2012).
14. Hritz, J., de Ruiter, A. & Oostenbrink, C. Impact of plasticity and flexibility on docking results for cytochrome P450 2D6: a combined approach of molecular dynamics and ligand docking. *J. Med. Chem.* **51**, 7469–7477 (2008).
15. Richter, L. *et al.* Diazepam-bound GABAA receptor models identify new benzodiazepine binding-site ligands. *Nature Chem. Biol.* **8**, 455–464 (2012).
16. Corbeil, C. R. & Moitessier, N. Docking ligands into flexible and solvated macromolecules. 3. Impact of input ligand conformation, protein flexibility, and water molecules on the accuracy of docking programs. *J. Chem. Inf. Model.* **49**, 997–1009 (2009).
17. Wei, B. Q., Weaver, L. H., Ferrari, A. M., Matthews, B. W. & Shoichet, B. K. Testing a flexible-receptor docking algorithm in a model binding site. *J. Mol. Biol.* **337**, 1161–1182 (2004).
18. Clauben, H., Buning, C., Rarey, M. & Lengauer, T. FlexE: efficient molecular docking considering protein structure variations. *J. Mol. Biol.* **308**, 377–395 (2001).
19. An, J. *et al.* A novel small-molecule inhibitor of the avian influenza H5N1 virus determined through computational screening against the neuraminidase. *J. Med. Chem.* **52**, 2667–2672 (2009).
20. Brooijmans, N. & Humblet, C. Chemical space sampling by different scoring functions and crystal structures. *J. Comput. Aid. Mol. Des.* **24**, 433–447 (2010).
21. Newman, J., Dolezal, O., Fazio, V., Caradoc-Davies, T. & Peat, T. The DINGO dataset: a comprehensive set of data for the SAMPL challenge. *J. Comput. Aid. Mol. Des.* **26**, 497–503 (2012).
22. Zhong, S. *et al.* Identification and validation of human DNA ligase inhibitors using computer-aided drug design. *J. Med. Chem.* **51**, 4553–4562 (2008).
23. Amaro, R. E. *et al.* Discovery of drug-like inhibitors of an essential RNA-editing ligase in *Trypanosoma brucei*. *Proc. Natl Acad. Sci. USA* **105**, 17278–17283 (2008).
24. Cheltsov, A. V. *et al.* Vaccinia virus virulence Factor N1L is a novel promising target for antiviral therapeutic intervention. *J. Med. Chem.* **53**, 3899–3906 (2010).
25. Sato, T. *et al.* Identification of novel drug-resistant EGFR mutant inhibitors by *in silico* screening using comprehensive assessments of protein structures. *Bioorg. Med. Chem.* **20**, 3756–3767 (2012).
26. Rogers, K. E. *et al.* Novel cruzain inhibitors for the treatment of Chagas' disease. *Chem. Biol. Drug Des.* **80**, 398–405 (2012).
27. Kumar, A. & Zhang, K. J. Computational fragment-based screening using RosettaLigand: the SAMPL3 challenge. *J. Comput. Aid. Mol. Des.* **26**, 603–616 (2012).
28. Bottegoni, G., Kufareva, I., Totrov, M. & Abagyan, R. Four-dimensional docking: a fast and accurate account of discrete receptor flexibility in ligand docking. *J. Med. Chem.* **52**, 397–406 (2008).
29. Armen, R. S., Chen, J. & Brooks, C. L. An evaluation of explicit receptor flexibility in molecular docking using molecular dynamics and torsion angle molecular dynamics. *J. Chem. Theory Comput.* **5**, 2909–2923 (2009).
30. Dietzen, M., Zotenko, E., Hildebrandt, A. & Lengauer, T. On the applicability of elastic network normal modes in small-molecule docking. *J. Chem. Inf. Model.* **52**, 844–856 (2012).
31. Vinh, N., Simpson, J., Scammells, P. & Chalmers, D. Virtual screening using a conformationally flexible target protein: models for ligand binding to p38alpha MAPK. *J. Comput. Aid. Mol. Des.* **26**, 409–423 (2012).
32. Barril, X. & Morley, S. D. Unveiling the full potential of flexible receptor docking using multiple crystallographic structures. *J. Med. Chem.* **48**, 4432–4443 (2005).
33. Afonine, P. V. *et al.* Joint X-ray and neutron refinement with phenix.refine. *Acta Crystallogr. D* **66**, 1153–1163 (2010).
34. Lang, P. T. *et al.* Automated electron-density sampling reveals widespread conformational polymorphism in proteins. *Protein Sci.* **19**, 1420–1431 (2010).
35. Shapovalov, M. V. & Dunbrack, R. L. Statistical and conformational analysis of the electron density of protein side chains. *Proteins: Struct. Funct. Bioinf.* **66**, 279–303 (2007).
36. Rosenfeld, R. J., Hays, A.-M. A., Musah, R. A. & Goodin, D. B. Excision of a proposed electron transfer pathway in cytochrome c peroxidase and its replacement by a ligand-binding channel. *Protein Sci.* **11**, 1251–1259 (2002).
37. Barelrier, S. *et al.* Roles for ordered and bulk solvent in ligand recognition and docking in two related cavities. *PLoS ONE* **8**, e69153 (2013).
38. Brenk, R., Vetter, S. W., Boyce, S. E., Goodin, D. B. & Shoichet, B. K. Probing molecular docking in a charged model binding site. *J. Mol. Biol.* **357**, 1449–1470 (2006).
39. Rocklin, G. J. *et al.* Blind prediction of charged ligand binding affinities in a model binding site. *J. Mol. Biol.* **425**, 4569–4583 (2013).
40. Wei, B. Q., Baase, W. A., Weaver, L. H., Matthews, B. W. & Shoichet, B. K. A model binding site for testing scoring functions in molecular docking. *J. Mol. Biol.* **322**, 339–355 (2002).
41. Coleman, R. G., Carchia, M., Sterling, T., Irwin, J. J. & Shoichet, B. K. Ligand pose and orientational sampling in molecular docking. *PLoS ONE* **8**, e75992 (2013).
42. Meng, E. C., Shoichet, B. & Kuntz, I. D. Automated docking with grid-based energy evaluation. *J. Comp. Chem.* **13**, 505–524 (1992).
43. Sharp, K. A. Polyelectrolyte electrostatics: salt dependence, entropic, and enthalpic contributions to free energy in the nonlinear Poisson–Boltzmann model. *Biopolymers* **36**, 227–243 (1995).
44. Irwin, J. J., Sterling, T., Mysinger, M. M., Bolstad, E. S. & Coleman, R. G. ZINC: a free tool to discover chemistry for biology. *J. Chem. Inf. Model.* **52**, 1757–1768 (2012).
45. Carlsson, J. *et al.* Ligand discovery from a dopamine D3 receptor homology model and crystal structure. *Nature Chem. Biol.* **7**, 769–778 (2011).
46. Mysinger, M. M. *et al.* Structure-based ligand discovery for the protein–protein interface of chemokine receptor CXCR4. *Proc. Natl Acad. Sci. USA* **109**, 5517–5522 (2012).
47. Rogers, D. J. & Tanimoto, T. T. A computer program for classifying plants. *Science* **132**, 1115–1118 (1960).
48. Berman, H. M. *et al.* The Protein Data Bank. *Nucleic Acid. Res.* **28**, 235–242 (2000).
49. Mysinger, M. M. & Shoichet, B. K. Rapid context-dependent ligand desolvation in molecular docking. *J. Chem. Inf. Model.* **50**, 1561–1573 (2010).
50. Gallagher, K. & Sharp, K. Electrostatic contributions to heat capacity changes of DNA–ligand binding. *Biophys. J.* **75**, 769–776 (1998).
51. Ytreberg, F. M. & Zuckerman, D. M. A black-box re-weighting analysis can correct flawed simulation data. *Proc. Natl Acad. Sci. USA* **105**, 7982–7987 (2008).

Acknowledgements

We thank G. Rocklin for enlightening discussions, P. Afonine for advice and bug fixing of the occupancy refinement in PHENIX, A. Doak for protein preparation and H. Lin, J. Karpiak and T. Balias for reading this manuscript. This work was supported by US National Institutes of Health grants GM59957 (B.K.S.), DP5OD009180 (J.S.F.) and NRSA F32GM096544 (R.G.C.).

Author contributions

M.F., R.G.C., J.S.F. and B.K.S. designed the study and wrote the paper, M.F. performed all experiments and refined structures with the assistance of J.S.F. R.G.C. wrote the computer code and performed all computational work.

Additional information

Supplementary information is available in the [online version](#) of the paper. Reprints and permissions information is available online at [www.nature.com/reprints](#). Correspondence and requests for materials should be addressed to J.S.F. and B.K.S.

Competing financial interests

The authors declare no competing financial interests.